IEEE Access
Multidisciplinary | Rapid Review | Open Access Journal

Received April 25, 2019, accepted July 16, 2019, date of publication July 29, 2019, date of current version August 13, 2019.

Digital Object Identifier 10.1109/ACCESS.2019.2931809

Improved Detection in Successive Interference Cancellation NOMA OFDM Receiver

HIND S. GHAZI AND KRZYSZTOF W. WESOŁOWSKI, (Member, IEEE)
Faculty of Electronics and Telecommunications, Poznań University of Technology, 60-965 Poznań, Poland

Corresponding author: Krzysztof W. Wesołowski (krzysztof.wesolowski@put.poznan.pl)

This work was supported by the Poznan University of Technology under Project DSMK/08/81/8125 and Project DSPB/08/81//8132.

ABSTRACT A successive interference cancellation receiver is one of the important blocks in non-orthogonal multiple access (NOMA) transmission. The quality of detection of the strongest user signals often decides about the quality of the whole system and minimizes the error propagation effect. In this paper, we propose an improved detection algorithm, which allows for using the NOMA transmission in a much smaller range of power differences between the terminals sharing common radio resources in the uplink, as compared with standard successive cancellation. The idea lies in the application of tentative decisions about weaker signals in the detection of stronger ones and then, after improved detection of stronger user signals, achieving more reliable decisions about the weaker ones. The simulation results reported in the paper confirm our idea, showing a much higher detection quality of the proposed receiver when compared with the standard solution.

INDEX TERMS Multi-carrier transmission, non-orthogonal multiple access, receiver, successive interference cancellation, uplink, WLAN.

I. INTRODUCTION

Typically, a wireless communication system is based on the orthogonality principle which ensures an assigned portion of frequency, time, or code resources for the exclusive use of a particular link between a terminal and a base station, between a terminal and an access point or between two terminals (as in the case of Device-to-Device (D2D) communications). Due to Orthogonal Multiple Access (OMA), signals from different links do not interfere with each other. This way, finite radio resources available to the given system are shared by many links simultaneously – though their number is strictly limited. Extremely high demands on traffic volume and data rates set by 5G system requirements [1] in the presence of very limited spectral resources caused a serious interest in loosening the assumptions about the orthogonality of the used resources, resulting in introducing Non-Orthogonal Multiple Access (NOMA) [2]–[5] and simultaneous use of the same resource units by more than one link. It is one of the techniques considered for application in 5G wireless communication systems although it was already proposed for the 4th generation LTE-Advanced system. Currently it is under consideration for 3GPP Release 16 standards of 5G systems (see 3GPP Technical Report TR 38.812 V16.0.0 "Study on Non-Orthogonal Multiple Access (NOMA) for NR" (Release 16)). We can easily imagine the application of NOMA in other communication systems, such as wireless LANs, Vehicle-to-Vehicle or Infrastructure communications (V2X), D2D communications, etc.

NOMA can be applied both in the downlink and uplink in the power domain or code domain. Fig. 1 presents the basic rules of NOMA signal reception in both directions [4] in the case of using the power domain. In the downlink, the base station (BS) applies lower power to the user facing better propagation conditions (User n) and higher power to the user who suffers from worse propagation conditions (User m). BS uses superimposed coding which enables the detection of signals directed to each user (m and n). In the uplink, the receiver of a base station first detects the strong signal, then reconstructs it in order to cancel it from the received signal. This enables the detection of the signal from the more distant and weaker user. In both cases Successive Interference Cancellation (SIC) is an important functional block of the receiver. The relative power levels for users sharing the same resources have been the subject of investigations [7], [9], [10].

Not much information can be found in the literature about the way the detection of subsequent users in the SIC block is performed, except for the fact that the user signals are

The associate editor coordinating the review of this manuscript and approving it for publication was Giovanni Pau.

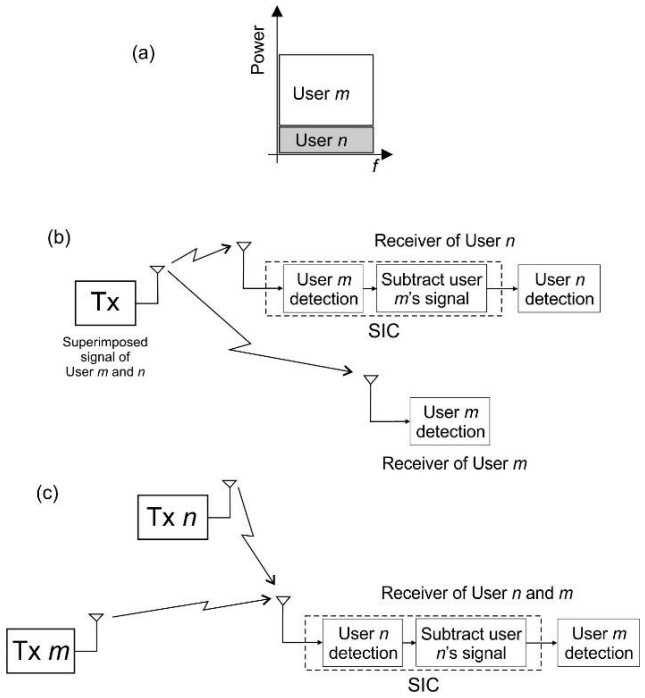

FIGURE 1. General NOMA model: Power assignment (a), downlink NOMA (b), uplink NOMA (c).

typically sorted from strongest to weakest and these signals are detected and cancelled subsequently. Typically, weaker users are treated as noise, although their signals differ substantially from an additive Gaussian noise, because their signals possess discrete probability density functions resulting from their discrete constellations. Thus, simple detection is far from optimum and can be performed only when differences in the power levels of subsequent users are sufficiently high. Otherwise, the error propagation effect prohibits such an operation.

The aim of this paper is to show on a simple example, how detection in the SIC receiver can be improved, which in turn leads to extending the range of power of constituent signals received by the SIC receiver.

The rest of this paper is organized as follows. In Section II we present the model of the considered system. We concentrate on the uplink direction. The role of the receiving station can be played by both a base station in a regular cellular system, an access point in WLAN, or a terminal in D2D transmission to which more than one transmission is directed. In Section III we overview a typical SIC detection algorithm and we introduce the proposed one, which substantially improves detection quality. We also propose a simple analysis of both detectors in Section IV. Section V contains a presentation of the simulation model and simulation results confirming the performance improvement due to the newly proposed detector. The paper ends with conclusions.

II. SYSTEM MODEL

For the purpose of presentation of our detector we consider an OFDM system operating in the uplink and shown in Fig. 2. Binary information block $\mathbf{x}^{(i)}$ $(i = 1, 2)$ given to the input

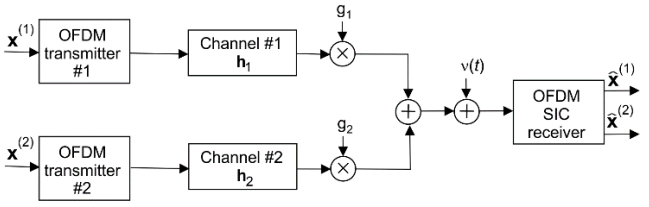

FIGURE 2. System model of the uplink NOMA applied in investigations.

of the OFDM transmitter is subject to channel coding and interleaving. Bits of the resulting codewords are mapped onto QPSK/QAM symbols that constitute subcarrier symbols of the IFFT modulator generating time domain samples supplemented by a cyclic prefix. Such sequences are subject to convolution with the baseband equivalent impulse response of the dispersive radio channel denoted by the vector $\mathbf{h}_i$ $(i = 1, 2)$. For simplicity we assume that the mean energy of each channel impulse response is normalized to unity. In order to model the propagation loss we assign the power P_i $(i = 1, 2)$ of signals incoming to the receiver from each user by setting the values of the coefficients $g_i = \sqrt{P_i}$. The received signal is disturbed by the additive white Gaussian noise $v(t)$. In the course of our paper we assume that signals from both transmitters arrive to the receiver with such a propagation delay difference that the receiver is able to select a common orthogonality period in which OFDM signals from both transmitters are analyzed. Typically, in D2D or V2X communications distances between transmitters and receivers are not large (e.g., up to a few hundred meters), so a coarse synchronization of both transmitters justifies such an assumption. For example, in the case of a typical IEEE 802.11 a/g/n WLAN, the transmission difference in the distance between a transmitter and the receiver equal to 200 m results in a propagation time difference lower than the length of the OFDM cyclic prefix equal to 0.8 μs.

Let us note that the OFDM SIC receiver selects a common orthogonality period for the sum of both incoming signals and performs FFT on it. Therefore, the signal on each OFDM subcarrier output (FFT bin) can be expressed by a simple equation:

$$Y_k = H_k^{(1)} X_k^{(1)} + H_k^{(2)} X_k^{(2)} + N_k \tag{1}$$

where $X_k^{(1)}$, $X_k^{(2)}$ are QPSK/QAM symbols transmitted on the k-th OFDM subcarrier $(k = 0, \ldots, N-1)$, $H_k^{(1)}$, $H_k^{(2)}$ are channel coefficients on this subcarrier, and

$$\mathbf{H}^{(i)} = \left[H_0^{(i)}, H_1^{(i)}, \ldots, H_{N-1}^{(i)}\right] = FFT\left\{g_i \mathbf{h}_i\right\}, \quad i = 1, 2 \tag{2}$$

N_k is a noise sample on the k-th subcarrier output.

Eq. (2) is fundamental for data detection on per-subcarrier basis using the SIC principle. Let us consider a standard solution resulting from the general rule shown in Fig. 1. In this approach, first, a strong component of the received signal is detected and the second and third components are jointly

treated as noise. Thus, the following operation is performed:

$$\widetilde{X}_k^{(1)} = \frac{Y_k}{\hat{H}_k^{(1)}} \quad \text{for } k = 0, 1, \ldots, N-1 \tag{3}$$

Based on the collected samples $\widetilde{X}_k^{(1)}$, $k = 0, 1, \ldots, N-1$, soft-decision demapping is typically performed, producing LLR (log-likelihood ratio) samples for each bit of the codeword of the channel code decoder. The result of channel decoding of the strong user (in our case #1) is the information sequence $\hat{\mathbf{x}}_1$. On its basis channel coding is performed again and QPSK/QAM remodulated symbols are produced, namely $\widehat{X}_k^{(1)}$, $(k = 0, 1, \ldots, N-1)$. They are subsequently used in the cancellation process, i.e., the weaker user data symbols are produced according to the following equation

$$\widetilde{X}_k^{(2)} = \frac{Y_k - \hat{H}_k^{(1)} \widehat{X}_k^{(1)}}{\hat{H}_k^{(2)}} \tag{4}$$

On the basis of the set of samples $\widetilde{X}_k^{(2)}$, $(k = 0, 1, \ldots, N-1)$ soft demapping is performed for the weaker user, producing LLR samples for the codeword bits of the channel code used by him. As a result, information block $\hat{\mathbf{x}}_2$ is generated.

Let us note that for making decisions and performing SIC cancellation, the knowledge of both channel coefficients is required. They have to be estimated on the basis of appropriately designed preambles or pilots purposely placed on the subcarrier–OFDM symbol grid. The particular implementation of the channel estimator depends on the applied system.

The existence of the weak signal certainly has a growing negative influence on the quality of the decisions about the strong user. We will show in our simulations that the power level difference between a strong and weak user is substantial to the reliable operation of the SIC receiver. It was the motivation to introduce an improved decision process which will extend the range of possible levels of a weaker user and enable reliable detection of both users in a large range of relative power levels.

III. PROPOSED DETECTION METHOD

Let us assume that the channel coefficients' true value or their estimates for weak and strong users are known due to the channel estimation process. Recall eq. (1) of the signal samples received in the FFT demodulator output. For the proposed receiver, tentative hard symbol-by-symbol decisions are first performed on both strong and weak signals concurrently, i.e., in conformance with the maximum likelihood (ML) criterion the following operation is performed

$$\left(\overline{X}_k^{(1)}, \overline{X}_k^{(2)}\right) = \arg \min_{X_k^{(1)}, X_k^{(2)}} \left| Y_k - \hat{H}_k^{(1)} X_k^{(1)} - \hat{H}_k^{(2)} X_k^{(2)} \right|^2$$

for

$$k = 0, 1, \ldots, N-1 \tag{5}$$

To get the tentative decisions according to (5) at this step we neglect the channel coding law which causes the dependence of QPSK/QAM symbols on each other. The main aim of performing (5) is to obtain $\overline{X}_k^{(2)}$ $(k = 0, 1, \ldots, N-1)$ which can be used for improving quality of samples of the FFT bins of the strong user. This time, instead of (3) we use the following samples to calculate the LLR values of codeword bits for the applied channel code by the strong user:

$$\widetilde{X}_k^{(1)} = \frac{Y_k - \hat{H}_k^{(2)} \overline{X}_k^{(2)}}{\hat{H}_k^{(1)}} \quad \text{for } k = 0, 1, \ldots, N-1 \tag{6}$$

After finding LLR soft-decision samples used in the channel decoder and deinterleaver, the final decision about information block $\hat{\mathbf{x}}_1$ of the strong user is made. Based on it, the codeword bits, interleaving and QPSK/QAM mappings are performed resulting in QPSK/QAM symbols $\widehat{X}_k^{(1)}$, $k = 0, 1, \ldots, N-1$. They are subsequently used in cancellation as in (4). As previously, on the basis of the set of samples $\widetilde{X}_k^{(2)}$, $(k = 0, 1, \ldots, N-1)$ soft demapping is performed for the weaker user, producing LLR samples for the codeword bits of the channel code used in this link. As a result, information block $\hat{\mathbf{x}}_2$ is generated.

Summarizing, the main improvement in the SIC cancellation lies in finding tentative decisions about weak user signals in (5) and using them in the calculation of strong user samples (6). Our simulation results shown in Section V indicate that this simple idea substantially improves the range of possible differences in power between strong and weak users.

Our proposal of SIC detector is illustrated in this paper on the example of two NOMA users. In general $K > 2$ users can be considered. For $K = 2$, additional complexity in comparison to the standard SIC detector results from searching for the best pair of data symbols received from the strong and weak user (see eq. (5)). The number of times when eq. (5) is implemented is $M_s M_w$ per OFDM active subcarrier where M_s and M_w are signal constellation sizes applied by the strong and weak user, respectively. In general, if there are K NOMA users each of them applying M-ary modulation on N subcarriers, the additional complexity over the standard SIC solution grows linearly with N and exponentially with M^K.

Our proposal can be extended for the NOMA system with $K > 2$ users in the following manner. Let the users be sorted in the descending power order. Then the first two strongest users are treated according to the proposed detection method whereas the remaining users are treated as distortion. If detection of both considered user data signals is successful, after reconstruction of both signals their influence can be cancelled from the joint received signal. The next pair of signals can be considered in the same manner. Such operation can be repeated till all of them are detected.

The authors of the paper are fully aware that much more sophisticated receivers can be considered for several scenarios of future 5G systems. Typically, they are well matched to particular transmission systems (spreading, channel coding, modulation size, etc.) and are usually based on iterative algorithms using minimum mean square error detectors, paral-

lel or serial interference cancellation, or more sophisticated detection algorithms such as elementary signal estimators (ESE), message passing algorithm (MPA) and expectation propagation algorithm (EPA). Despite that we limit our considerations to a simple case of SIC detector for which the proposed detector improvement can be easily evaluated.

IV. SIMPLIFIED THEORETICAL ANALYSIS OF TWO SIC DETECTORS

In order to justify our proposed improved detector, let us analyze two simplified cases. In the first one, the traditional SIC detector described mainly by equations (3) and (4) is considered, whereas in the second one we analyze the proposed SIC detector (equations (5), (6) and (4)). An example of a similar analysis performed for the traditional SIC detector can be found in [14]. Our analysis is simpler, but leads to fully analytical results. In both cases we omit the fact that typically channel coding is applied, as otherwise, the analysis would be much more complicated. We also consider signals on a single subcarrier and for the simplicity of our analysis we take the following equation describing a signal on the FFT output (we neglect the subcarrier number for the clarity of our notation):

$$Y = Y^R + jY^I = X_1 + gX_2 + \nu \tag{7}$$

Let us assume that data symbols X_1 and X_2 are QPSK modulated and are selected from the set $\{A + jA, -A + jA, A - jA, -A - jA\}$. Coefficient g is the weighting factor of magnitude not larger than unity. In general, it can be complex, however, let us assume for simplicity that it is real (no phase shift is observed between the stronger X_1 and weaker X_2 (due to g) signals). Let both data symbols be statistically independent and equiprobable. Let us also assume that ν is a sample of the white zero mean Gaussian noise of variance σ^2.

A. ERROR PROBABILITY ANALYSIS OF REGULAR SIC DETECTOR

First, let us calculate the symbol error probability for the strong receiver aiming at the detection of X_1 symbols. Recall that it makes a direct decision about X_1 on the basis of the received sample Y (7). Denote $P_C(X_1)$ as the probability of correct reception for a particular symbol X_1. Denote $P(X_1)$ as the probability of generation of X_1. Clearly, on the basis of our assumptions, $P(X_1) = 1/4$ for each data symbol X_1. Then the symbol error probability $P_E^{(1)}$ for a stronger signal can be described by the equation

$$P_E^{(1)} = 1 - \sum_{X_1} P_C(X_1)P(X_1) \tag{8}$$

where

$$P_C(X_1) = \sum_{X_2} P_C(X_1|X_2)P(X_2) \tag{9}$$

Consider the particular data symbol $X_1 = A + jA$. Let us introduce variables b_1^R and b_1^I in the form

$$b_1^R = A + gX_2^R \tag{10}$$

$$b_1^I = A + gX_2^I \tag{11}$$

which constitute the in-phase and quadrature components of both received signals without noise, respectively (each of the X_2 data symbol components are equal to $X_2^R = \pm A$, $X_2^I = \pm A$). Taking into account that the in-phase and quadrature noise components have variance $\sigma^2/2$, we can write

$$P_C(X_1|X_2) = \left(1 - \frac{1}{2}\text{erfc}\left(\frac{b_1^R}{\sigma}\right)\right)\left(1 - \frac{1}{2}\text{erfc}\left(\frac{b_1^I}{\sigma}\right)\right) \tag{12}$$

Therefore, recalling that for other symbols X_1 the situation is fully analogous, and $P(X_1) = P(X_2) = 1/4$, we get the final result:

$$\begin{aligned} P_E^{(1)} &= 1 - \frac{1}{4}\sum_{X_2}\left(1 - \frac{1}{2}\text{erfc}\left(\frac{b_1^R}{\sigma}\right)\right)\left(1 - \frac{1}{2}\text{erfc}\left(\frac{b_1^I}{\sigma}\right)\right) \\ &= 1 - \frac{1}{4}\left[2 - \frac{1}{2}\left(\text{erfc}\left(\frac{A+gA}{\sigma}\right) + \text{erfc}\left(\frac{A-gA}{\sigma}\right)\right)\right]^2 \end{aligned} \tag{13}$$

Let us note that the presence of signal X_2 in sample Y substantially influences the error probability for data symbol X_1. Fig. 3 illustrates formula (13) for several values of the weighting coefficient g.

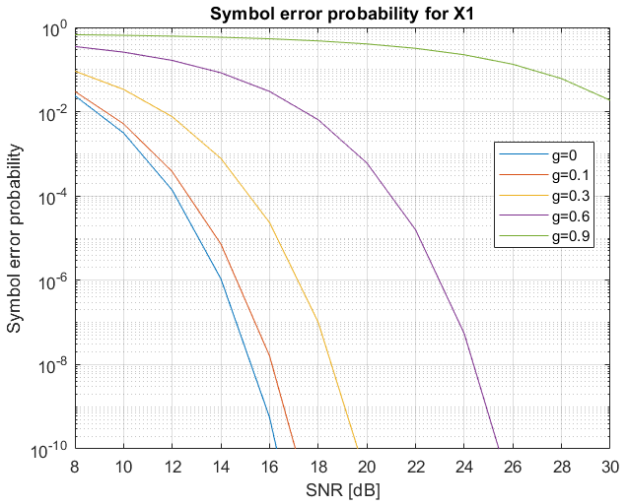

FIGURE 3. Symbol error probability according to (13) for model (7).

Now let us focus our attention on the symbol error probability for the weaker received signal. First, let us calculate the probability for a correct decision made for symbol X_2. It can be expressed in the form

$$\begin{aligned} P_C(X_2) = \sum_{X_1}\Big[&P_C(X_2|\text{correct}\,\widehat{X}_1)(1 - P_E^{(1)}) \\ &+ P_C(X_2|\text{incorrect}\,\widehat{X}_1)P_E^{(1)}\Big]\,P(X_1) \end{aligned} \tag{14}$$

Certainly,

$$P_E^{(2)} = 1 - \sum_{X_2} P_C(X_2)P(X_2) \tag{15}$$

Consider $P_C(X_2|\text{correct}\,\widehat{X}_1)$ first. The SIC detector cancels X_1 correctly by subtracting $\widehat{X}_1 = X_1$ from Y, so after cancellation we get

$$Z = Y - \widehat{X}_1 = gX_2 + \nu \tag{16}$$

In order to apply the threshold detector to X_2 we have to divide both sides of (16) by g, therefore we receive

$$Z' = X_2 + \frac{\nu}{g} \tag{17}$$

Consider the signal $X_2 = A + jA$ as the transmitted one. For this case, knowing that $\nu = \nu^R + j\nu^I$ we have

$$\begin{aligned} P_C(X_2 &= A + jA|\text{correct}\,\widehat{X}_1) \\ &= \Pr\left\{\frac{\nu^R}{g} > -A\right\}\Pr\left\{\frac{\nu^I}{g} > -A\right\} \\ &= \left[1 - \frac{1}{2}\text{erfc}\left(\frac{Ag}{\sigma}\right)\right]^2 \end{aligned} \tag{18}$$

It is worth noting again that for the remaining QPSK-modulated X_2 symbols the situation is analogous, resulting in the same expression for the correct conditional decision (18). Therefore,

$$P_C(X_2|\text{correct}\,\widehat{X}_1) = \left[1 - \frac{1}{2}\text{erfc}\left(\frac{Ag}{\sigma}\right)\right]^2 \tag{19}$$

In the case of incorrect detection of X_1, calculations are substantially more complicated. In [14] the authors simplify their similar considerations of error calculations for multiuser detectors when a stronger signal is wrongly detected, indicating that the error propagation has a disruptive effect on the weaker signal reception quality and the conditional probability $P_C(X_2|\text{incorrect}\,\widehat{X}_1)$ can be well approximated by 1/4 (in the case of QPSK) due to a virtually equally probable guess of the data symbol $\widehat{X}_2$.Therefore, recalling that all symbols X_1 are equally probable, we can express (14) in the form

$$P_C(X_2) = \left[1 - \frac{1}{2}\text{erfc}\left(\frac{Ag}{\sigma}\right)\right]^2 (1 - P_E^{(1)}) + \frac{1}{4}P_E^{(1)} \tag{20}$$

Substituting (20) in (15) we finally obtain:

$$P_E^{(2)} = 1 - \left[1 - \frac{1}{2}\text{erfc}\left(\frac{Ag}{\sigma}\right)\right]^2 (1 - P_E^{(1)}) - \frac{1}{4}P_E^{(1)} \tag{21}$$

B. ERROR PROBABILITY ANALYSIS FOR THE PROPOSED SIC DETECTOR

As already mentioned, in our analysis we do not take into account the fact that channel coding is typically applied for both links, and we assume that symbol-by-symbol detection is performed at the receiver. According to our proposal, first the detector attempts to find a tentative decision about the weaker symbol X_2. In order to do it, it selects such a pair $(\overline{X}_1, \overline{X}_2)$ that minimizes the metric shown below, which is a simplified version of metric (5).

$$(\overline{X}_1, \overline{X}_2) = \arg\min_{X_1, X_2} |Y - X_1 - gX_2|^2 \tag{22}$$

A correct guess $\overline{X}_2$ about X_2 will presumably result in decreasing $P_E^{(1)}$ when the final decision about X_1 is calculated and it will also have a positive impact on the error probability of the weaker signal.

As previously, we can write

$$P_E^{(1)} = 1 - \sum_{X_1} P_C(X_1)P(X_1)$$

but in the current case

$$\begin{aligned} P_C(X_1) = P_C(X_1|\text{correct}\,\overline{X}_2)\Pr\left\{\text{correct}\,\overline{X}_2\right\} \\ + P_C(X_1|\text{incorrect}\,\overline{X}_2)\left(1 - \Pr\left\{\text{correct}\,\overline{X}_2\right\}\right) \end{aligned} \tag{23}$$

Let us start our calculations with deriving the expression for $\Pr\{\text{correct}\,\overline{X}_2\}$. This calculation is rather straightforward, but cumbersome. Let us assume again that $X_1 = A + jA$. The consideration of all other possible symbols X_1 leads to identical results. Fig. 4 presents all areas in which the end of the noise vector has to be placed when the tentative decision $\overline{X}_2$ is correct and decisions related to X_1 and X_2 are found according to (22). Such considerations have to be made for each correct symbol X_2. In the sequel we show only one such calculation for $X_2 = -A + jA$ presented in Fig. 4. All the remaining values of X_2 can be considered similarly and these calculations will be omitted.

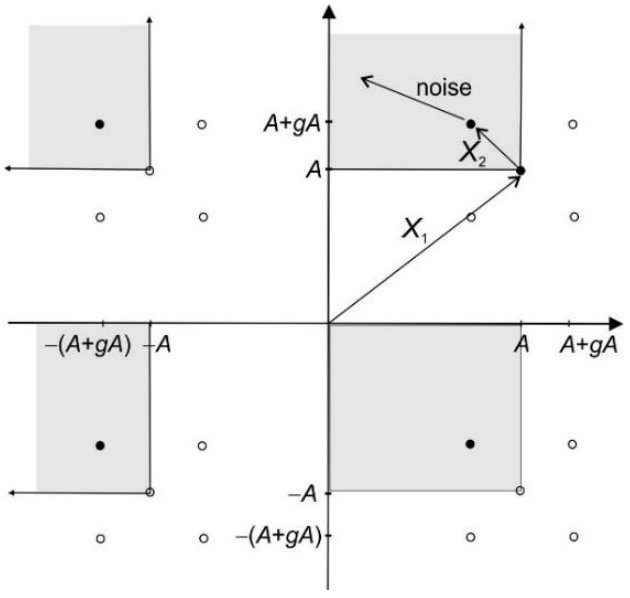

FIGURE 4. Areas determining correct decisions based on (22) about $X_2 = -A + jA$ when $X_1 = A + jA$.

For the case shown in Fig. 4 we have

$$\begin{aligned} &\Pr\left\{\text{correct}\,\overline{X}_2|X_1 = A + jA,\ X_2 = -A + jA\right\} \\ &= \left(\frac{1}{\sqrt{\pi}\sigma}\int_{-(A-gA)}^{gA} e^{-\frac{t^2}{\sigma^2}}dt\right)\cdot\left(\frac{1}{\sqrt{\pi}\sigma}\int_{-gA}^{\infty} e^{-\frac{t^2}{\sigma^2}}dt\right) \end{aligned}$$

$$+\left(\frac{1}{\sqrt{\pi}\sigma}\int_{-\infty}^{-(2A-gA)} e^{-\frac{t^2}{\sigma^2}}dt\right)\cdot\left(\frac{1}{\sqrt{\pi}\sigma}\int_{-gA}^{\infty} e^{-\frac{t^2}{\sigma^2}}dt\right)$$
$$+\left(\frac{1}{\sqrt{\pi}\sigma}\int_{-\infty}^{-(2A-gA)} e^{-\frac{t^2}{\sigma^2}}dt\right)\cdot\left(\frac{1}{\sqrt{\pi}\sigma}\int_{-(2A+gA)}^{gA} e^{-\frac{t^2}{\sigma^2}}dt\right)$$
$$+\left(\frac{1}{\sqrt{\pi}\sigma}\int_{-(A-gA)}^{gA} e^{-\frac{t^2}{\sigma^2}}dt\right)\cdot\left(\frac{1}{\sqrt{\pi}\sigma}\int_{-(2A+gA)}^{-(A+gA)} e^{-\frac{t^2}{\sigma^2}}dt\right) \quad (24)$$

The upper and lower borders in the integrals of (24) result from the values of in-phase and quadrature noise components which have to occur to made a correct decision about X_2. These calculations lead to the following result:

$$\begin{aligned}\Pr\left\{\text{correct}\,\overline{X}_2|X_1 = A+jA,\ X_2 = -A+jA\right\} &= \left[1-\frac{1}{2}\text{erfc}\left(\frac{A-gA}{\sigma}\right)-\frac{1}{2}\text{erfc}\left(\frac{gA}{\sigma}\right)\right.\\ &\left.+\frac{1}{2}\text{erfc}\left(\frac{2A-gA}{\sigma}\right)\right]\\ &\times\left[1-\frac{1}{2}\text{erfc}\left(\frac{2A+gA}{\sigma}\right)-\frac{1}{2}\text{erfc}\left(\frac{gA}{\sigma}\right)\right.\\ &\left.+\frac{1}{2}\text{erfc}\left(\frac{A+gA}{\sigma}\right)\right]\end{aligned}$$

Considering similarly all the remaining three data symbols X_2, knowing that they are equiprobable ($P(X_2) = 1/4$), we end up with the following formula for $\Pr\{\text{correct}\,\overline{X}_2\}$:

$$\begin{aligned}\Pr\left\{\text{correct}\,\overline{X}_2\right\} = \frac{1}{4}\left\{2-\text{erfc}\left(\frac{gA}{\sigma}\right)\right.&\\ -\frac{1}{2}\left[\text{erfc}\left(\frac{A-gA}{\sigma}\right)-\text{erfc}\left(\frac{A+gA}{\sigma}\right)\right]&\\ \left.+\frac{1}{2}\left[\text{erfc}\left(\frac{2A-gA}{\sigma}\right)-\text{erfc}\left(\frac{2A+gA}{\sigma}\right)\right]\right\}^2 &\quad (25)\end{aligned}$$

Returning to (23) it is easy to show that the probability of correct reception of X_1 under the condition of the correct tentative decision $\overline{X}_2$ is simply equal to the probability of the correct reception of the QPSK signal in the presence of additive Gaussian noise, so

$$P_C(X_1|\text{correct}\,\overline{X}_2) = \left[1-\frac{1}{2}\text{erfc}\left(\frac{A}{\sigma}\right)\right]^2 \quad (26)$$

Now let us turn our attention to the calculation of $P_C(X_1|\text{incorrect}\,\overline{X}_2)$. We can write the following expression in which $\overline{X}_2$ is again a decision about transmitted X_2:

$$P_C(X_1|\text{incorrect}\,\overline{X}_2) = \sum_{X_2} P_C(X_1|\text{incorrect}\,\overline{X}_2, X_2)P(X_2) \quad (27)$$

In this case calculations are even more lengthy, but still manageable. We consider again $X_1 = A + jA$ and all possible transmitted X_2 symbols. Considerations for all other X_1 symbols are analogous. For each X_2 the incorrect decision $\overline{X}_2$ has three possible forms that have to be taken into account. After lengthy calculations similar to those resulting from Fig. 4 we end up with the formula:

$$\begin{aligned}P_C(X_1|\text{incorrect}\,\overline{X}_2) = (Ca+Db)\,[(Ca+Db)&\\ +2B(2-a-b)]&\quad (28)\end{aligned}$$

where

$$B = 1-\frac{1}{2}\text{erfc}\left(\frac{A}{\sigma}\right),\quad C = 1-\frac{1}{2}\text{erfc}\left(\frac{A+2gA}{\sigma}\right)$$
$$D = 1-\frac{1}{2}\text{erfc}\left(\frac{A-2gA}{\sigma}\right) \quad (29)$$

and

$$\begin{aligned}a &= \frac{1}{2}\text{erfc}\left(\frac{gA}{\sigma}\right)-\frac{1}{2}\text{erfc}\left(\frac{A+gA}{\sigma}\right)+\frac{1}{2}\text{erfc}\left(\frac{2A+gA}{\sigma}\right)\\ b &= \frac{1}{2}\text{erfc}\left(\frac{gA}{\sigma}\right)+\frac{1}{2}\text{erfc}\left(\frac{A-gA}{\sigma}\right)-\frac{1}{2}\text{erfc}\left(\frac{2A-gA}{\sigma}\right)\end{aligned} \quad (30)$$

Using (23), (25), (28) – (30) we are able to plot the error probability for symbol X_1. It turns out the error probability curves as functions of SNR for several coefficient values g are the same as in Fig. 3. It was also confirmed by Monte Carlo simulation of the system described by (7). This means that using the modified detector in such a simple scheme as considered in this section does not bring any advantages. As the error probability for X_1 is the same as in the regular detector, the same holds true for X_2 and formula (21) is further valid. However, as we will see, simulations performed for channel coded systems prove that a substantial improvement in the performance of the proposed SIC detector is possible as compared with the regular one. The explanation of this fact is the following. By application of the tentative decision $\overline{X}_2$ in detection of X_1, the receiver is able to calculate more reliable soft LLR values used at the input of the channel code decoder applied in X_1 link. More errors are corrected as compared with the traditional detector with symbol-by-symbol cancellation and LLRs calculated on its basis. Thus, the regenerated sequence of X_1 symbols contains fewer errors and in consequence, it results in a lower error probability of X_2 after the cancellation of the whole block of $\widehat{X}_1$ symbols.

Unfortunately, an analysis of the system with channel coding would be much more complicated, and therefore we resort to simulations.

V. SIMULATION RESULTS

We have checked the quality of the proposed SIC detection algorithm on the example of a standard IEEE 802.11a system based on the WiFi model analyzed in [12]. In our experiments the system consisted of two users co-operating with an access point. It could also be a model of two terminals sharing common resources and communicating with another terminal in D2D fashion. Let us note that such a model can also be

applied in V2V communications where a system very similar to 802.11a, namely IEEE 802.11p, still prevails. In Table I the main parameters of the modelled IEEE 802.11a system are recalled for convenience.

TABLE 1. Basic Parameters of IEEE 802.11a System.

Parameter	Value
Bandwidth	20 MHz
Cyclic prefix duration	0.8 µs
Data duration	3.2 µs
FFT size	64
No. of subcarriers	52
Operating frequency band	5 GHz
Sampling rate	40 MHz
Subcarrier spacing	312.5 KHz
Throughput	6 up 54 Mbps
Total symbol duration	4.0 µs

As we have already mentioned, OFDM symbols that are transmitted from both terminals are quasi-synchronous, i.e., the receiver is able to find the orthogonality period needed for OFDM symbol detection, which is located within OFDM symbols generated by each terminal. The convolutional code is used at the transmitting side with coding rate (R = 1/2). The standard (133,171) code is applied. Different modulation schemes are applied depending on the channel propagation path of each user. Therefore, 16-QAM or QPSK are used in simulation experiments for strong and weak users, respectively. Other modulation choices and coding rates, i.e., modulation and coding schemes (MCS) are also possible, depending on individual channel conditions. Applied channel models were simulating multipath Rayleigh fading channels denoted in the text by vectors $\mathbf{h}_1$ and $\mathbf{h}_2$ and they had exponential decay power profile with selected rms delay spread.

A. SYSTEM PERFORMANCE WITH IDEAL CHANNEL COEFFICIENTS

To verify the detection quality of the proposed algorithm in comparison to the regular one, first, ideal channel coefficients knowledge is assumed. This shows improvements in detection abilities of the algorithm itself.

In the simulation experiments the number of packets that was transmitted from each terminal was $K = 100$, 500 or 1000, depending on the required accuracy and level of BER estimation. Every packet contained $L = 100$ payload OFDM symbols. The simulation results consist of two different parts.

The first part shows the estimated bit error rate (BER) vs. signal-to-noise ratio (SNR) measurements for both users when the rms delay spread was set to be $T_{rms} = 50$ ns. In the second part the rms delay spread was $T_{rms} = 100$ ns. In all our simulation runs we assume the following definition of SNR:

$$SNR = 10\log_{10}\left(\frac{P_{Tx}(g_1^2 + g_2^2)}{N}\right) \tag{31}$$

where P_{Tx} is the reference transmitted power by both terminals, N is the noise power and the channel coefficients g_1 and g_2 model both propagation loss and change of the power level with respect to the reference one. In all simulation results shown below we set $g_1 = 1$ without the loss of generality.

A multipath channel model typical for WiFi was applied [12]. The power delay profile was exponentially decaying, depending on the root mean square delay T_{rms}. The energy of the channel impulse response was normalized to unity to better control power by selecting the weighting coefficients g_2. We assumed the time invariance of the channel impulse response within a packet.

Fig. 5 shows the results of these experiments for the stronger terminal which applied 16QAM. It is clearly seen that the regular SIC detector works for relatively low values of the strength of a weak signal only. For $g_2 = 0.3$ the BER curve for the strong user is already almost flat and BER does not diminish with increasing SNR anymore. Detection quality of the proposed SIC detector certainly deteriorates with the growth of the relative strength of the weak signal, but the system still works even if the $g_2 = 1$. This is equivalent to the case when the power of the weaker signal is in fact the same as the stronger one.

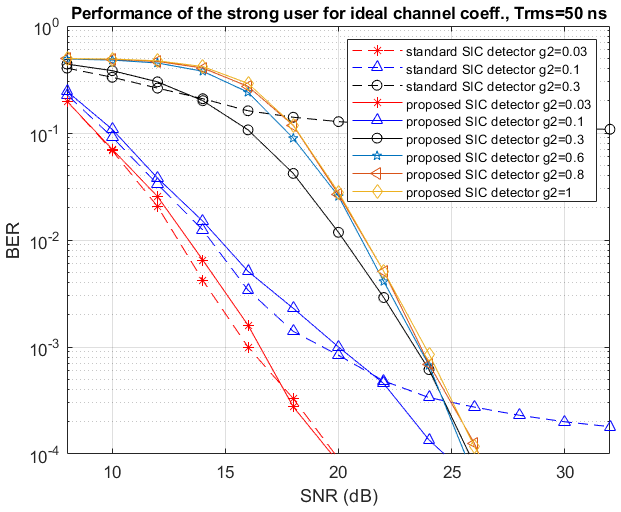

FIGURE 5. Performance of the received data transmitted by the strong terminal for several levels (g_2) of the weak signal ($T_{rms} = 50$ ns) when ideal channel coefficients are applied.

Fig. 6 presents the BER versus SNR plots for the weaker terminal which transmits data using QPSK modulation. The conclusion which can be drawn from this figure is basically the same. The proposed SIC detector operates at much higher powers of the weaker terminal as compared with the stronger one, therefore, it is much more reliable. For the lowest selected power of the weaker signal ($g_2 = 0.03$) it cannot be received in the reasonable range of SNR, as the practical SNR for it is too low to operate reliably. However, already for $g_2 = 0.1$ reception is possible, although it requires higher SNR.

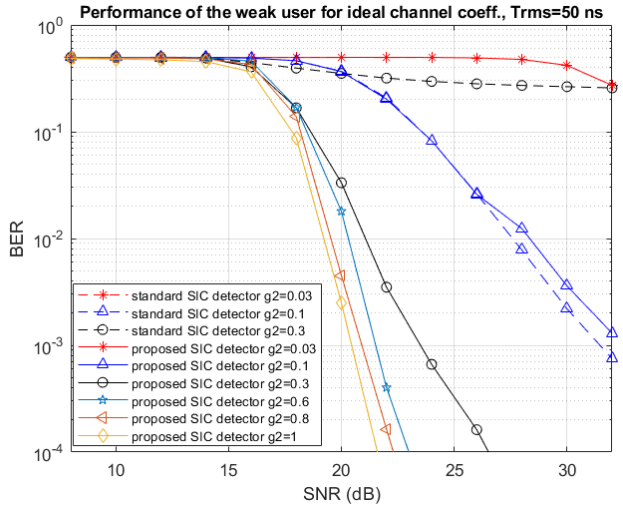

FIGURE 6. Performance of the received data transmitted by the weak terminal for several levels (g_2) of the weak signal (T_{rms} = 50 ns) when ideal channel coefficients are applied.

Similar experiments have been performed when the channel delay spread was T_{rms} = 100 ns. A more demanding channel, as compared with the previous one, results in a similar BER performance. It is shown in Figs. 7 and 8.

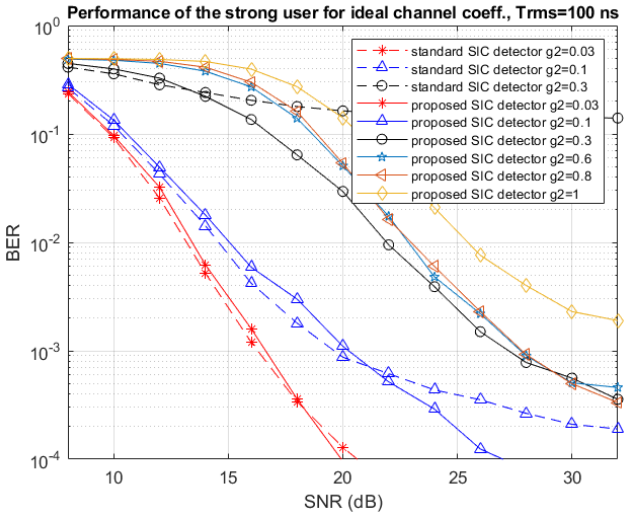

FIGURE 7. Performance of the received data transmitted by the strong terminal for several levels (g_2) of the strong signal (T_{rms} = 100 ns) when ideal channel coefficients are applied.

We can draw similar conclusions as in the case of a very low rms time spread channel. Again, the regular SIC detector operates in the limited range of relative power of the weak signal, whereas the proposed detector can operate in the whole range of values, even in the case of equal power of signals arriving from both terminals.

B. SYSTEM PERFORMANCE WITH ESTIMATED CHANNEL COEFFICIENTS

In the next set of experiments the channel coefficients in the frequency domain were estimated and the resulting estimates were used in the detection process in both regular and

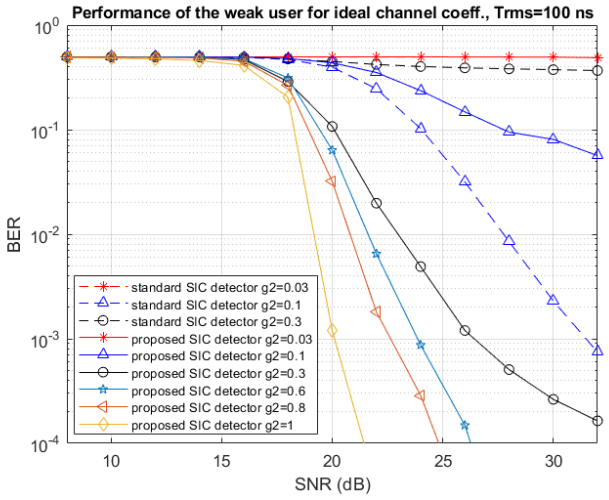

FIGURE 8. Performance of the received data transmitted by the weak terminal for several levels (g_2) of the weak signal (T_{rms} = 100 ns) when ideal channel coefficients are applied.

proposed SIC detectors. As IEEE 802.11a transmission is not fitted to NOMA operation, we propose a simple method of channel estimation for both users in the form of the short packet exchange at the start of NOMA operation. Such a procedure can be repeated in appropriate time intervals if needed, because of the variability of channel characteristics. Fig. 9 shows the scheme of such an operation. First, terminal #1 transmits a short packet consisting of a preamble only. Then, terminal #2, after a passive reception of the preamble from terminal #1, transmits its own preamble as well. After that, the access point transmits the START signal and NOMA operation begins when both terminals transmit their packets concurrently. Initially, channel estimation for both links was based on a standard procedure using two long training sequences of the 802.11a/g preamble. As the samples of both long training symbols are known, the received FFT outputs being the response of the channel to both training symbols

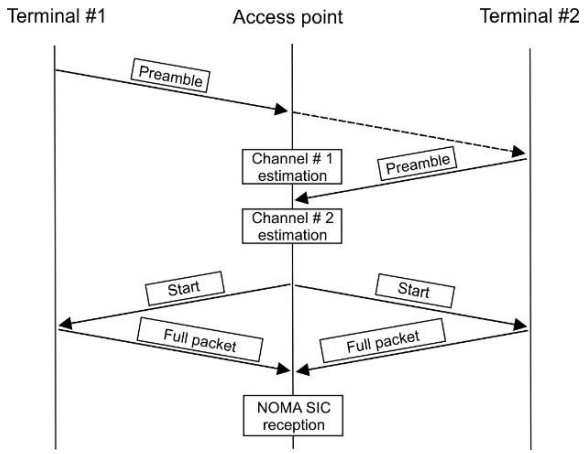

FIGURE 9. Proposed procedure for initial channels' estimation and NOMA operation.

were averaged and subsequently divided by the ideal tones of both training symbols [12].

However, our experiments indicate that in the case of SIC operation, precise knowledge of both channel characteristics is crucial for the detection process. Direct use of the preamble only causes a serious deterioration in the performance as compared with the ideal knowledge of the channel characteristics. We have performed experiments in which the proposed SIC detector used not only two reference symbols in the 802.11a preamble but also some following OFDM symbols acting as additional pilot symbols.

Figs. 10 and 11 show how much we can gain by lengthening the preamble by a few following OFDM pilot symbols. The plots are done for a strong and weak user, respectively. The gain in the performance is clearly visible. We can see that when sufficiently long channel testing packets are applied, the deterioration in the BER performance is about 1 dB as compared with the case of using the ideal coefficients. Certainly, too long preamble causes the loss in the transmission efficiency, so some kind of a compromise has to be selected. In the case of using estimated coefficients, we applied $N_p = 6$ pilot symbols (including the OFDM symbols C1 and C2, already contained in the preamble).

Figs. 12, 13, 14 and 15 show the BER performance for the system with T_{rms} channel spread equal to 50 and 100 ns when $N_p = 6$ pilot OFDM symbols have been applied.

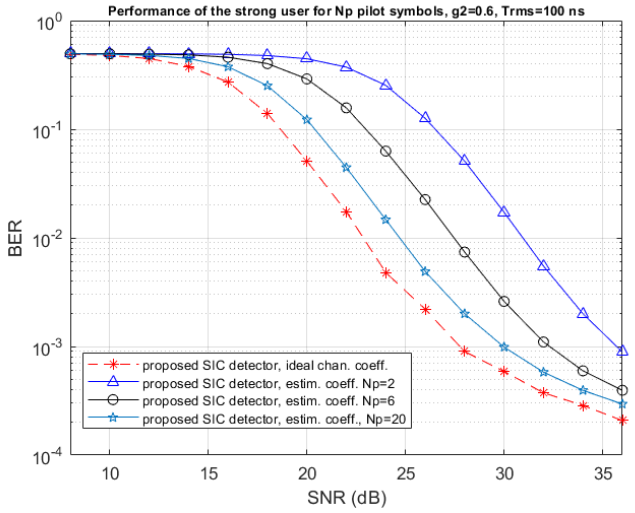

FIGURE 10. BER for proposed SIC detector for the strong user depending on the number of OFDM pilot symbols N_p compared with the performance when ideal channel coefficients are applied.

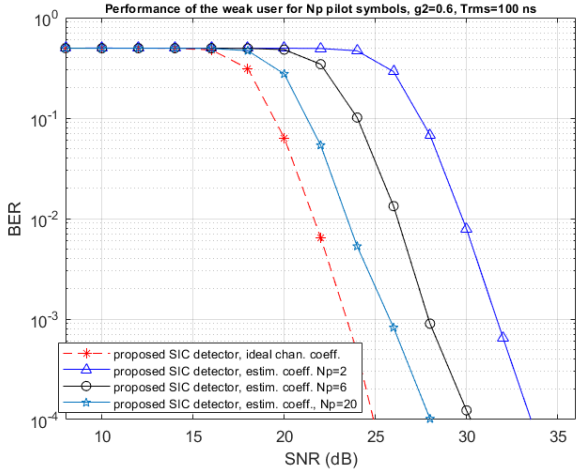

FIGURE 11. BER for proposed SIC detector for the weak user depending on the number of OFDM pilot symbols N_p compared with the performance when ideal channel coefficients are applied.

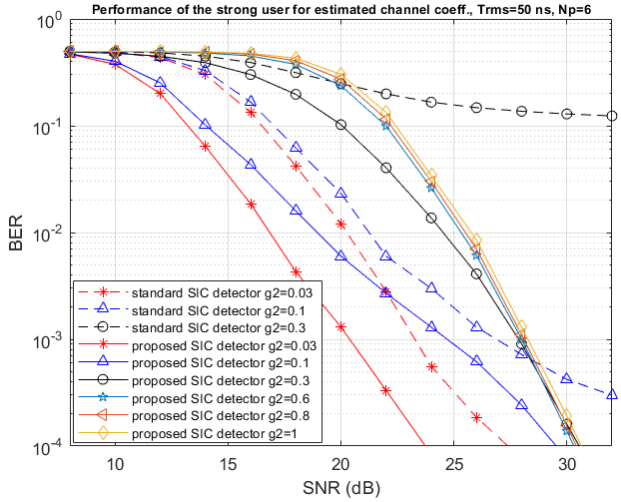

FIGURE 12. BER of the received data transmitted by the strong terminal for several levels (g_2) of the weak signal (T_{rms} = 50 ns) when estimated channel coefficients are applied

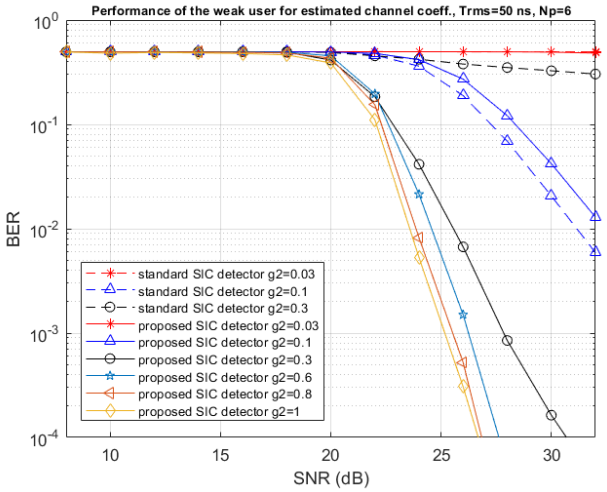

FIGURE 13. BER of the received data transmitted by the weak terminal for several levels (g_2) of the weak signal (T_{rms} = 50 ns) when estimated channel coefficients are applied.

VI. DISCUSSION ON MAC ISSUES

NOMA operation within the WiFi standard has certainly not been foreseen yet. Thus, substantial changes in MAC (medium access control) procedures should be made which

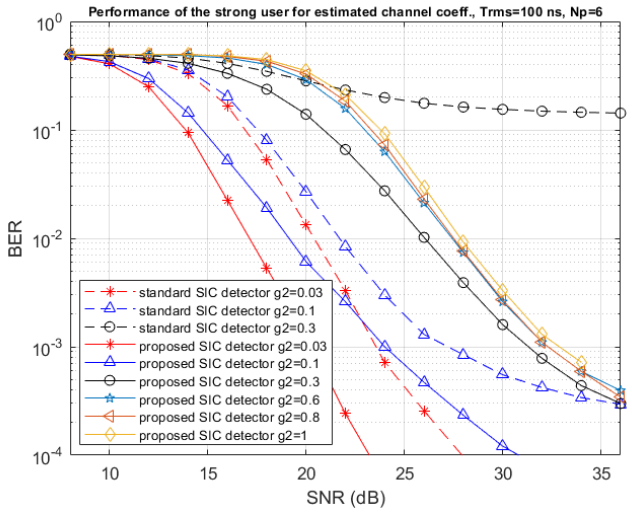

FIGURE 14. BER of the received data transmitted by the strong terminal for several levels (g_2) of the weak signal (T_{rms} = 100 ns) when estimated channel coefficients are applied.

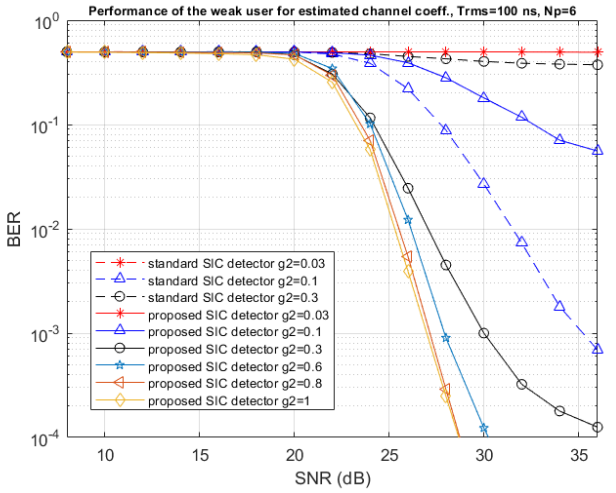

FIGURE 15. BER of the received data transmitted by the weak terminal for several levels (g_2) of the weak signal (T_{rms} = 100 ns) when estimated channel coefficients are applied.

enable uplink transmission of two terminals at the same time. An additional issue is the pairing of appropriate terminals which differ in the received power in the access point. This problem is much easier to solve when the proposed SIC detector is applied instead of the regular one. However, in our opinion, research on alternative MAC algorithms enabling NOMA is worth consideration, as using WiFi in the NOMA mode enables a substantial increase in data throughput.

Another potential application of the proposed SIC detector is data exchange in physical layer network coding (PNC) [13]. In regular operation of PNC, after receiving a sequence of symbols in the multiple access phase, joint symbols from both terminals are interpreted in order to transmit the modulo-2 sum of the received bits. This way, hard decisions have to be made without taking into account channel coding, which is usually applied. Instead of this operation, each data stream after detection using the applied SIC detector can be recovered, including error correction decoding, and then the bit-by-bit modulo-2 sum of information blocks could be re-encoded and transmitted to both terminals in the broadcast phase, enabling the reception of the data stream from the remote terminal with much higher quality.

VII. CONCLUSION

Intensive simulations performed for regular and proposed SIC detectors applied in NOMA arrangement and shown on the example of a traditional IEEE 802.11a system have proven that the proposed detector can be a valuable alternative to the regular one and it substantially extends the range of relative powers of the NOMA users. This approach can be applied to other systems in which access to the transmission medium is based on methods different from CSMA (carrier-sense multiple access). Another possible application of the proposed detector is Physical Layer Network Coding. A system of that kind will be the subject of our future research.

REFERENCES

[1] P. Marsch, Ö. Bulakçi, O. Queseth, and M. Boldi, Eds., *5G System Design: Architectural and Functional Considerations and Long Term Research*. Chichester, U.K.: Wiley, 2018.

[2] Y. Yuan, "Non-orthogonal multi-user superposition and shared access," in *Signal Processing for 5G: Algorithms and Implementations*, F.-L. Luo and C. J. Zhang, Eds. Chichester, U.K.: Wiley, 2016, pp. 116–142.

[3] A. Benjebbour, K. Saito, A. Li, Y. Kishiyama, and T. Nakamura, "Non-orthogonal multiple access (NOMA): Concept and design," in *Signal Processing for 5G: Algorithms and Implementations*, F.-L. Luo and C. J. Zhang, Eds. Chichester, U.K.: Wiley, 2016, pp. 143–168.

[4] Y. Liu, Z. Qin, M. Elkashlan, Z. Ding, A. Nallanathan, and L. Hanzo, "Nonorthogonal multiple access for 5G and beyond," *Proc. IEEE*, vol. 105, no. 12, pp. 2347–2389, Dec. 2017. doi: 10.1109/JPROC.2017.2768666.

[5] J. Zeng, T. Lv, R. P. Liu, X. Su, M. Peng, C. H. Wang, and J. Mei, "Investigation on evolving single-carrier NOMA into multi-carrier NOMA in 5G," *IEEE Access*, vol. 6, pp. 48268–48288, 2018. doi: 10.1109/ACCESS.2018.2868093.

[6] H. Kayama and H. Jiang, "Evolution of LTE and new radio access technologies for FRA (future radio access)," in *Proc. 48th Asilomar Conf. Signals, Syst. Comput.*, Nov. 2014, pp. 1944–1948.

[7] R. Al Faeik, K. Davaslioglu, and R. Gitlin, "The optimum received power levels of uplink non-orthogonal multiple access (NOMA) signals," in *Proc. IEEE 18th Wireless Microw. Technol. Conf. (WAMICON)*, Apr. 2017, pp. 1–4.

[8] H. S. Ghazi and K. Wesolowski, "Uplink NOMA scheme for Wi-Fi applications," *Int. J. Electron. Telecommun.*, vol. 64, no. 4, pp. 481–485, 2018. doi: 10.24425/123549.

[9] Z. Wei, D. W. K. Ng, and J. Yuan, "Power-efficient resource allocation for MC-NOMA with statistical channel state information," in *Proc. IEEE Global Commun. Conf. (GLOBECOM)*, Washington, DC, USA, Dec. 2016, pp. 1–7. doi: 10.1109/GLOCOM.2016.7842161.

[10] C.-L. Wang, J.-Y. Chen, and Y.-J. Chen, "Power allocation for a downlink non-orthogonal multiple access system," *IEEE Wireless Commun. Lett.*, vol. 5, no. 5, pp. 532–535, Oct. 2016. doi: 10.1109/LWC.2016.2598833.

[11] R. Sun, Y. Wang, X. Wang, and Y. Zhang, "Transceiver design for cooperative non-orthogonal multiple access systems with wireless energy transfer," *IET Commun.*, vol. 10, no. 15, pp. 1947–1955, 2016. doi: 10.1049/iet-com.2016.0120.

[12] A. Schwarzinger, *Digital Signal Processing in Modern Communication Systems*. Lake Mary, FL, USA: Andreas Schwarzinger, 2013.

[13] U. Bhat and T. M. Duman, "Decoding strategies at the relay with physical-layer network coding," *IEEE Trans. Wireless Commun.*, vol. 11, no. 12, pp. 4503–4513, Dec. 2012.
[14] G. J. M. Janssen and S. B. Slimane, "Symbol error probability analysis of a multiuser detector for M-PSK signals based on successive cancellation," *IEEE J. Sel. Areas Commun.*, vol. 20, no. 2, pp. 330–338, Feb. 2002.

HIND S. GHAZI was born in Baghdad, Iraq, in 1982. She received the B.Sc. and M.Sc. degrees in communication engineering from the University of Technology, Iraq, in 2004 and 2007, respectively. She is currently pursuing the Ph.D. degree in information and communication technologies with the Poznań University of Technology, Poland. She has worked as an Assistant Lecturer at the Communication Engineering Department, Al-Mamon University College, Baghdad, Iraq. Her research interests include 5G systems and wireless communications.

KRZYSZTOF W. WESOŁOWSKI was born in Wolsztyn, Poland, in 1952. He received the M.Sc. degree in electrical engineering from the Poznań University of Technology, Poznań, in 1976, the M.Sc. degree in mathematics from Adam Mickiewicz University, Poznań, in 1977, and the Ph.D. degree in telecommunication engineering from the Poznań University of Technology, in 1982.

From 1982 to 1989, he was an Assistant Professor with the Poznań University of Technology; from 1989 to 1999, he was an Associate Professor; and since 1999, he has been a Full Professor with the Faculty of Electrical Engineering and later at the Faculty of Electronics and Telecommunications, since 2006. He is the author of two books published by John Wiley & Sons entitled *Introduction to Digital Communication Systems* and *Mobile Communication Systems* and more than 150 articles. His research interests include digital signal processing for digital and wireless communication systems, channel coding, and information theory.

Prof. Wesołowski was a recipient of the scholarships funded by the Fulbright Foundation (Northeastern University, Boston, USA) and the Alexander von Humboldt Foundation (University of Kaiserslautern, Germany). His research team participated in several European Union funded projects devoted to development of wireless systems and networks, including 5G (7FP EU METIS project), nationally funded projects, and his team cooperated with international and Polish industry.